Role of extruded sheet morphology in phase separation and final morphology of superhydrophobic polypropylene

Vámos Cs., Varga L. J., Marosfői B., Bárány T.

Accepted for publication in Periodica Polytechnica-Mechanical Engineering
Published in 2022
DOI: 10.3311/PPme.20509

 https://doi.org/10.3311/PPme.20509
Creative Commons Attribution

Periodica Polytechnica Mechanical Engineering, 66(3), pp. 260–271, 2022

Role of Extruded Sheet Morphology in Phase Separation and Final Morphology of Superhydrophobic Polypropylene

Csenge Vámos[1,2*], László József Varga[1], Botond Marosfői[2], Tamás Bárány[1]

[1] Department of Polymer Engineering, Faculty of Mechanical Engineering, Budapest University of Technology and Economics, Műegyetem rkp. 3., 1111 Budapest, Hungary
[2] Furukawa Electric Institute of Technology Ltd, Késmárk utca 28/A., 1158 Budapest, Hungary
* Corresponding author, e-mail: csenge.vamos@furukawaelectric.com

Received: 22 May 2022, Accepted: 01 June 2022, Published online: 24 June 2022

Abstract

In this study, we prepared polypropylene sheets with a superhydrophobic surface from extruded sheets with a phase separation method. We investigated the influence of extrusion parameters on the morphological properties of the polypropylene sheet and found that two significantly different structures can be formed in the cross-section of the sheet when the cooling temperature was varied. The effect of the morphology of the extruded material was studied on phase separation and through that on the surface structure that formed. The created morphology of the extruded sheet plays a significant role in the procedure of the phase separation method and less in surface wettability. We also included a polypropylene blend and nucleated polypropylene in this study to investigate their role in surface morphological changes and indirectly on wetting behavior. Surfaces have become superhydrophobic with an increased water contact angle from 102° to 150° and contact angle hysteresis below 10°. For nucleated polypropylene samples, we achieved remarkably good results (a water contact angle of 158°). The morphological and wettability behavior of the surfaces were investigated with a polarized optical microscope and water contact angle measurements, and scanning electron microscopy, respectively.

Keywords

superhydrophobic polymeric surfaces 1, extrusion parameters 2, phase separation method 3, nucleated PP, PP blend 4

1 Introduction

In the past few decades, superhydrophobic surfaces have been gaining significant attention within different scientific and industrial fields [1, 2]. The importance of the research topic is well illustrated by the increasing amount of research on these surfaces [3]. Conventionally, the applied methods for creating superhydrophobic surfaces are classified into two approaches, namely creating the rough surface and modification of the chemical composition of the surface with a material having low surface energy [4]. Developing a simple, controllable, and inexpensive method for large-scale superhydrophobic surfaces is still a great challenge [5], since the currently available techniques consist of multiple steps to achieve the final product and require specific equipment and time-consuming processes [6].

The solvent-based techniques, including phase separation methods, can address these needs [7, 8] since phase separation is a widely used technique to prepare superhydrophobic surfaces on semi-crystalline polymers, such as polypropylene (PP) [9]. During the phase separation method, a homogeneous solution is first prepared with polymer and a high-boiling point solvent at an elevated temperature to create a homogeneous solution. Then the phase separation is induced by cooling the polymer solution or adding non-solvent to the solution [9].

As a result, phase separation takes place so that a roughened structure will be obtained from the separated phases after the evaporation of the solvent. The polymer contributes to the formation of a matrix structure that can be tuned by the interactions between polymers and solvent and the polymer/solvent ratio [9].

Superhydrophobic surfaces made from PP have been studied by several authors due to the intrinsically hydrophobic nature of PP and their great price–performance ratio [10]. First, Erbil et al. [11] reported on superhydrophobic PP surfaces using the phase separation method with the appropriate selection of solvents, non-solvents, and cooling temperatures.

Cite this article as: Vámos, C., Varga, L. J., Marosfői, B., Bárány, T. "Role of Extruded Sheet Morphology in Phase Separation and Final Morphology of Superhydrophobic Polypropylene", Periodica Polytechnica Mechanical Engineering, 66(3), pp. 260–271, 2022. https://doi.org/10.3311/PPme.20509

Surface wettability is closely related to the morphology of the surface formed with phase separation. Numerous researchers have studied the effect of solvents and the crystallization behavior of PP in surface structure formation during phase separation [12, 13].

In the case of non-nucleated PP grades, the course of crystallization depends on the regularity of the chain structure and the crystallization conditions [14]. Zhu et al. [15] systematically studied the effect of the tacticity of PP on surface wettability by changing the mass ratio of the composite coatings of atactic and isotactic PP. The created surface was water repellent and wetting behavior could be tuned from slippery to sticky with a change of the ratio of atactic and isotactic PP. The distinct wetting behaviors can be attributed to the different morphologies, which resulted from the different crystallization behaviors of PP with different regularity.

We can also find an example of constructing superhydrophobic PP surfaces with the addition of a nucleating agent. The distribution and size of spherulites and the rate of phase separation can be influenced with nucleating agents, which can be inorganic and organic materials like salts, fillers, organic acids, polymers and apolar materials soluble in the molten polymer [16, 17]. The structure of superhydrophobic surfaces made from solutions is influenced by the polymerization catalyst. Zhang et al. [18] investigated superhydrophobic surfaces made of metallocene catalyst PP (m-PP) and Ziegler–Natta catalyst PP (ZN-PP). Depending on the type of catalyst, the micro-sized particles formed on the surface differed. A micro-sized crystalline particle formed on the surface of the m-PP film, while the ZN-PP particle surface exhibited an amorphous state. They found that during film formation, m-PP had a higher crystallization rate and higher crystallinity. The results also revealed that the superhydrophobicity and thermal stability of the m-PP film were much better than those of the ZN-PP film.

Several studies have reported the potential of superhydrophobic surfaces produced from polymer blends [19, 20]. Rioboo and coworkers have shown that it is possible to tune the superhydrophobicity of polymer surfaces by simply modifying the ratio of non-superhydrophobic and superhydrophobic polymers in the blend. They also revealed that superhydrophobic coating could be produced from commercial PP, including recycled materials [19].

PP is one of the most widely used polymers in many commodities as well as industrial applications [21, 22]. Injection molding and extrusion are among the most common processing techniques used to produce PP products [23, 24]. In both processing technologies, the morphology of the products shows a strong correlation with the applied processing technology [25–27]. Liparoti et al. [28] investigated the morphological and structural differences caused by mold temperature in injection molded samples. Examination of the cross-sections revealed that different polymer layers with different crystallinity and orientation were formed due to the different cooling temperatures of the mold. By varying the temperature of the mold, they were able to modify the thickness of each layer or even eliminate the layer.

During extrusion, the temperature of the caliber unit, as well as the drawing ratio, play a major role in the cross-sectional morphological properties and mechanical characteristics of the resulting samples [27, 29].

Macauley et al. [27] studied the correlations between the structural properties of extruded PP sheets and the extrusion parameters. They concluded that the morphology of the extruded sheets is primarily influenced by caliber temperature. Both the crystallinity and the thickness of the lamella show a decreasing tendency with decreasing caliber temperature and with increasing supercooling. As a result of the increasing supercooling, the cross-section of the sheets can be divided into two very different regions by the abruptly cooling outer part in contact with the caliber and the spherulitic bulk structure formed inside the sheet.

Most phase separation methods form the structured surface from a polymer solution by coating [30–32]. Fewer examples can be found of using the phase separation method to create a structured surface from the bulk material. One can assume that the morphology of extruded material might affect phase separation and, through that ,the surface structure formed. In this study, we investigated the effect of the morphology of extruded sheets on the phase separation method and on the surface characteristics by its wetting properties. We also included samples containing minor polymer components or nucleating agents in this study to investigate their role in surface morphological changes and indirectly on wetting behavior.

2 Materials and methods

2.1 Materials

We used Tipplen H681F polypropylene homopolymer (MOL Petrolkémia Zrt., Tiszaújváros, Hungary) as matrix material, which has a melt flow rate of 1.7 g/10 min (measured at the temperature of 230 °C with the load of 2.16 kg). We used two different propene-rich grades of atactic poly-

alpha olefins (APAOs), kindly proided by Evonik (Evonik Resource Efficiency GmbH, Marl, Germany) sold under the tradenames of Vestoplast® 703 (VP 703) and Vestoplast® 792 (VP 792). The properties of the APAO grades are listed in Table 1.

We also used a non-soluble nucleating agent, ADK STAB NA-21E (Adeka, Tokyo, Japan). It is an aluminum-containing organophosphorus compound with a melting point of 210 °C. As a solvent, we used xylene (mixture of isomers, purity 98%) supplied by VWR Chemicals, Germany.

2.2 Sample preparation

First, a PP sheet with a thickness of 1 mm was extruded with a co-rotating twin-screw extruder (TSA, Cernobbio, Italy, L/D ratio 40, D = 32 mm) equipped with a 150 mm wide sheet die. The die lip gap was set to 2.5 and 1.1 mm. The temperature zones were set to 190, 200, 200, 200 and 200 °C from hopper to die, and the die temperature was 210 °C. The screw speed was 60 1/min. As caliber and conveying equipment, vertical cylinders (Trocellen QCAL-Quadro Calandra Linea R&G) were used. The temperatures of the cylinders were 30 °C and 80 °C, and the pulling speed was set according to the final 1 mm thickness of the sheet.

We prepared the nucleated PP in two extrusion steps. For the nucleated samples, a masterbatch with 1 wt% was added to the PP and dry-mixed in advance, and extruded with a co-rotating twin-screw extruder, with a rod die. The temperature zones were set to 190, 200, 200, 200 and 200 °C from hopper to die, and the temperature of the die was 200 °C, and screw speed was 20 1/min. The extruded masterbatch filaments were pelletized with an S330 granulator (Rapid, Bredaryd, Sweden) and added to the PP pellets. The final nucleating agent concentration was 500 ppm. The nucleated PP was sheet-extruded with similar settings to the neat PP. However, in the case of nucleated PP, we only worked with a cylinder temperature of 80 °C and a die lip gap of 1.1 mm.

We also prepared neat PP sheets by film extrusion. The sheets were prepared with a LE 25-30/C single-screw extruder and an LCR300 flat-film line (Labtech Engineering Co. Ltd., Samutprakarn, Thailand). The temperatures of the extruder zones were 190, 195, 200, 205 and 210 °C from hopper to die, and the die temperature was 210 °C. The lips of the die were opened to 2 mm. Sheets were prepared with cylinder temperatures of 30 and 80 °C at two different screw speeds. In one case, the screw speed was 280 1/min with a pulling speed of 1.0 m/min and in the other case, the screw speed was 300. 1/min with 1.4 m/min pulling speed.

Table 1 Main properties of the APAO grades

Name	Melt viscosity at 190 °C (Pa s)	Molecular weight, Mw (g/mol)	Tensile strength (MPa)
Vestoplast® 703	2.7 ± 0.7	34 000	2.1
Vestoplast® 792	120 ± 30	118 000	5.8

The polymer blends were prepared in two extrusion steps. At first, the dry mixture of PP and APAO was extruded into a filament with a LE 25-30/C co-rotating twin-screw extruder (Labtech Engineering Co. Ltd., Samutprakarn, Thailand). The weight ratio of PP and APAO was 90/10. The rotating speed of the volumetric feeder was 30 1/min, and the temperature of the extruder zones was 190, 195, 200, 200, 200, 205, 205, 210, 210 and 210 °C from hopper to die, the temperature of the die was 210 °C, and screw speed was 120 1/min. The extruded filaments were pelletized with an LZ-120/VS granulator (Labtech Engineering Co. Ltd., Samutprakarn, Thailand). As a second step, a sheet was prepared with settings similar to those used in the film extrusion of neat PP. For polymer blends, we only used a cylinder of 80 °C and the pulling speeds of 1.0 m/min.

The nominated thickness of the extruded sheet, regardless of the type of extruder, was 1 mm.

The schematic diagram of the two types of extruders used can be seen in Fig. 1.

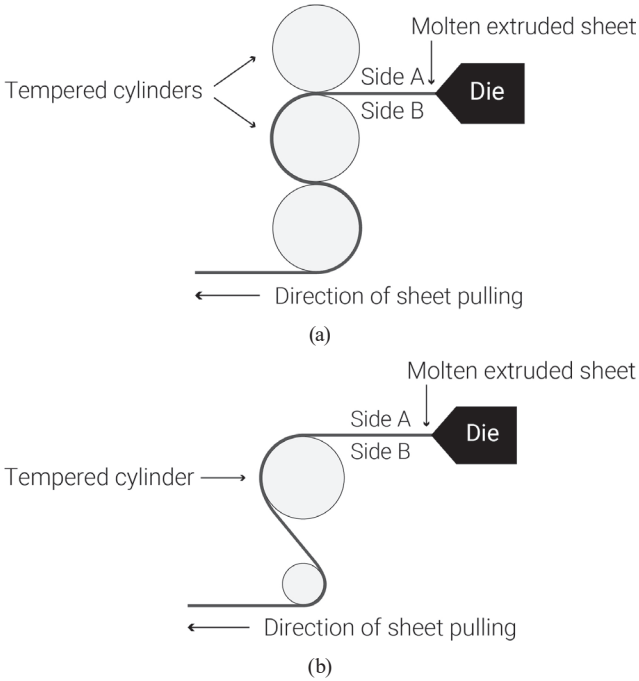

Fig. 1 Schematic diagram of the arrangement of tempered cylinders of sheet extrusion (a) and film extrusion (b)

For phase separation, we cut the samples from the extruded sheets and immersed them in a xylene bath for 60 s at 125 °C. Finally, the samples were dried at 30 °C for 24 hours in an air-ventilated oven (UT6120, Thermo Fischer Scientific, USA), then 24 hours in a vacuum oven (FCD-3000, Faithful) at 30 °C. After the drying step, the skin layers were peeled off from both sides of the sheet and the peeled sheets were used for further investigation.

2.3 Morphology characterization

The surface and cross-sectional morphology were analyzed with a scanning electron microscope (SEM) (Jeol JSM-IT 200). For the cross-sectional examination, samples were cryo-fractured under liquid nitrogen and sputtered with a thin gold layer for 50 s with 10 mA in a vacuum using a sputter coater (JEOL JFC-1300 Auto Fine Coater).

The melting behavior of the samples was examined by differential scanning calorimetry (DSC12E, Mettler- Toledo) in a nitrogen atmosphere. For the analysis, the samples were heated at 10 °C/min from 30 to 220 °C. This temperature was maintained for 5 minutes and then the samples were cooled to 30 °C at a cooling rate of 10 °C/min. The degree of crystallinity (X_c) was determined according to Eq. (1).

$$X_c = \left(\frac{\Delta H_m}{\Delta H_0} \right) \times 100 \,, \tag{1}$$

where X_c is the degree of crystallinity of PP, ΔH_m is the first melting enthalpy and ΔH_0 is the melting enthalpy for a 100% crystalline sample; for PP it is 207 J/g [33].

A Zeiss Axioscope polarized optical microscope (POM) equipped with a Leica DFC 320 digital camera was used to visualize the structural layer over the thickness of the extruded samples.

The water contact angle was measured with a sessile water drop with a Ramé-Hart model 100-06 contact angle measuring system at ambient temperature. First, a 20 µl droplet of distilled water was gently deposited onto the surface of the sample. The homogeneity of the surface was characterized by contact angle hysteresis, which is the difference between the advancing and receding contact angles obtained from the droplet construction and removal procedure. Contact angle measurement data were evaluated with the Image J software.

Tensile tests were performed with a Z020 universal tensile testing machine (Zwick/Roell GmbH, Ulm, Germany) equipped with a 20 kN load cell. The test speed was 200 mm/min, and the initial grip-to-grip separation was 20 mm. The tests were conducted at room temperature (23 °C), and at least 5 five specimens were tested in each case.

The peeling test was performed using a Z010 universal tensile testing machine (Zwick/Roell GmbH, Ulm, Germany) equipped with a 10 kN load cell. For the tests, 50 × 120 mm^2 rectangular specimens were used. The skin layer on the samples was glued with adhesive tape (466, Tesa, Germany, Hamburg) the end of the adhesive tape was secured between the grips of the tensile machine, and the sample was placed in a standard roller holder used for the tear test. The test was performed at a speed of 1000 mm/min. The tear force was measured as a function of the elongation. The test was carried out on 5 specimens in each case.

3 Results

In order to vary the cross-sectional morphology of the samples, we used two extrusion methods for sample preparation. Table 2 contains the list of the prepared samples with the main settings. The S/PP/30/1 suffix refers to the type of extrusion, the material used, the temperature of the cooling cylinder, and the velocity of pulling.

A POM study was carried out to determine the cross-sectional morphology of the samples. The morphological structure over the cross-section of the extruded samples with respect to the cooling temperature and the pulling velocity is shown in Fig. 2. Fig. 2 (a)–(d) presents the POM images of sheets cooled with symmetric cylinder arrangement and Fig. 2 (e)–(h) presents POM images of sheets cooled with asymmetric cylinder arrangement.

Based on the POM images, we can establish that different preparation methods result in samples with different cross-sectional morphology. On the one hand, we were able to produce samples Fig. 2 (a)–(d) that had a symmetrical cross-sectional structure due to contact by tempered rollers on both sides. Cooling was the same on both sides of the extruded samples. On the other hand, by applying the asymmetrical cooling technique (tempered roller and room temperature air), we can get samples Fig. 2 (e)–(h) with asymmetrical shell-core morphology in the cross-section.

Table 2 The extrusion settings and sample designations

Designation	Type of extrusion	Cylinder temperature (°C)	Pulling velocity (m/min)
S/PP/30/1	symmetric	30	1.0
S/PP/80/1		80	1.0
S/PP/30/1.3		30	1.3
S/PP/80/1.3		80	1.3
A/PP/30/1	assymetric	30	1.0
A/PP/80/1		80	1.0
A/PP/30/1.4		30	1.4
A/PP/80/1.4		80	1.4

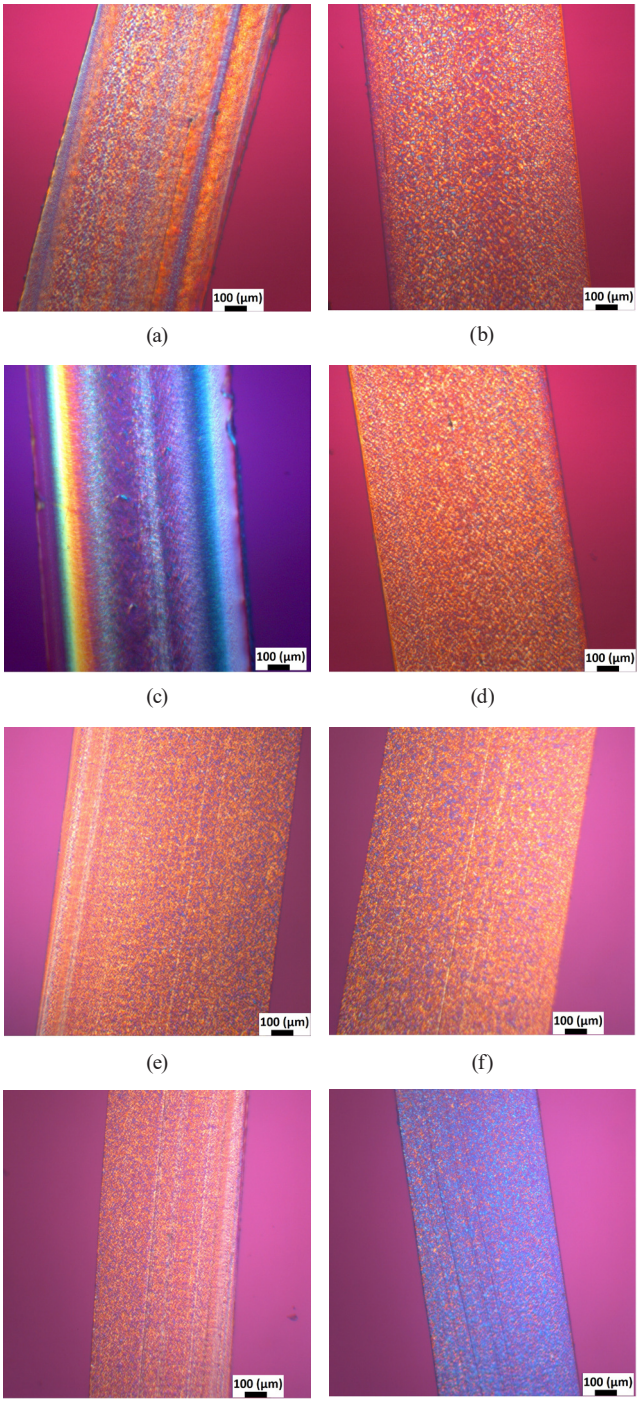

Fig. 2 POM images of extruded PP sheets, where (a) is S/PP/30/1, (b) is S/PP/80/1, (c) is S/PP/30/1.3, (d) is S/PP/80/1.3, (e) is A/PP/30/1, (f) is A/PP/80/1, (g) is A/PP/30/1.4 and (h) is A/PP/80/1.4

The thick core layer is composed of spherulites, which are formed under quiescent-like crystallization conditions. The high cooling rate of 30 °C near the shell layer leads to the formation of a highly oriented structure. Furthermore, a high-resolution analysis would be needed if we wanted to differentiate the sublayers.

Lowering the cooling rates by increasing the cooling temperature to 80 °C leads to a very thinshell layer since the oriented macromolecules have a longer time for relaxation. For samples having an asymmetrical structure, no shell layer formed on the non-contacting side . Presumably, the cooling rate of this side was slower, similar to the side cooled at 80 °C; the polymer molecules were able to crystallize in the form of spherulites. We compared the crystallinity of the extruded samples by DSC and established no significant differences (37–39%) in the degree of crystallinity with different sample preparation methods.

The extruded samples were solvent-treated according to the schematic graph in Fig. 3.

The solvent treatment is based on temperature-induced phase separation and revealed several morphological changes in the PP samples, as shown in the SEM images in Fig. 4 (a) and (b). The solvent swells the surface region to a depth of several tens of micrometers, increasing chain mobility. When the solvent evaporates, it causes recrystallization and a porous structure (see Fig. 4 (a)). In addition to the solvent-affected layer on the sample surface, another structure appears, denoted as the "skin layer", which can be peeled off from the treated sheet samples. As shown below (Fig. 4 (a)), the skin layer is compact and the solvent-affected layer beneath is porous. As the solvent gradually diffuses toward the center of the material, it forms a gradient structure. The recrystallized spherulites are large and close to the surface, and their size gradually decreases toward the center.

We examined the samples by SEM to compare the morphologies after the solvent immersion and drying process. Fig. 5 shows the results of the evaluation of cross-sectional SEM micrographs of the samples, the thickness of skin and the porous layer as a function of cooling temperature. Both sides of the samples were evaluated, and it is represented as side A and side B. The same color (blue or red) belongs to the same side of the sample.

Samples S/PP/30/1 and S/PP/30/1.3 have a symmetrical structure after extrusion. After solvent treatment, the thickness of the skin and porous layers on both sides of the samples is nearly the same. The samples A/PP/30/1 and A/PP/30/1.4 have asymmetric structures; the thickness of the skin and the porous layer are not equal on opposite sides of the samples. The A and B sides of samples S/PP/30/1 and S/PP/30/1.3 and the B side of samples A/PP/30/1 and A/PP/30/1.4 were tempered in a similar way (in contact with the cylinder at 30 °C), and the thicknesses of the skin and porous layer are nearly identical. The air-contact side

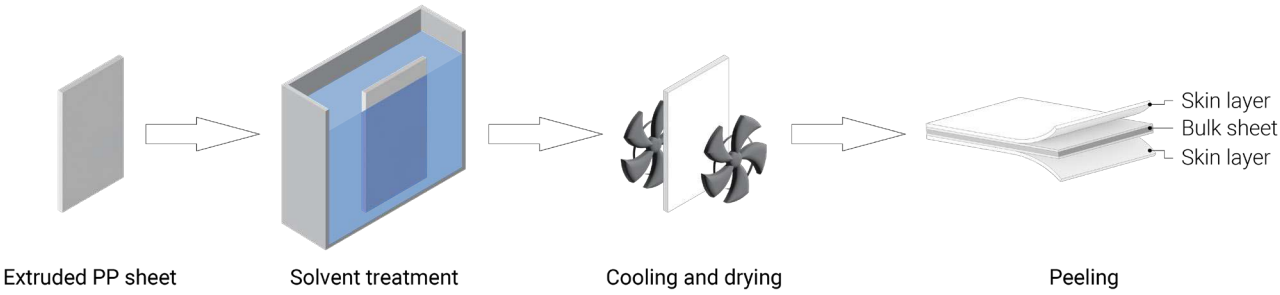

Fig. 3 Schematic graph of solvent treatment

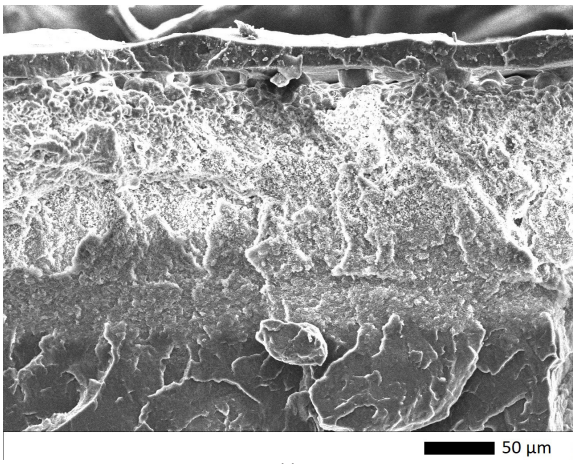

(a)

(b)

Fig. 4 SEM micrographs of a solvent-treated PP sample, (a) cryo-fractured cross-section close to the surface and (b) upper view of the surface after skin layer removal

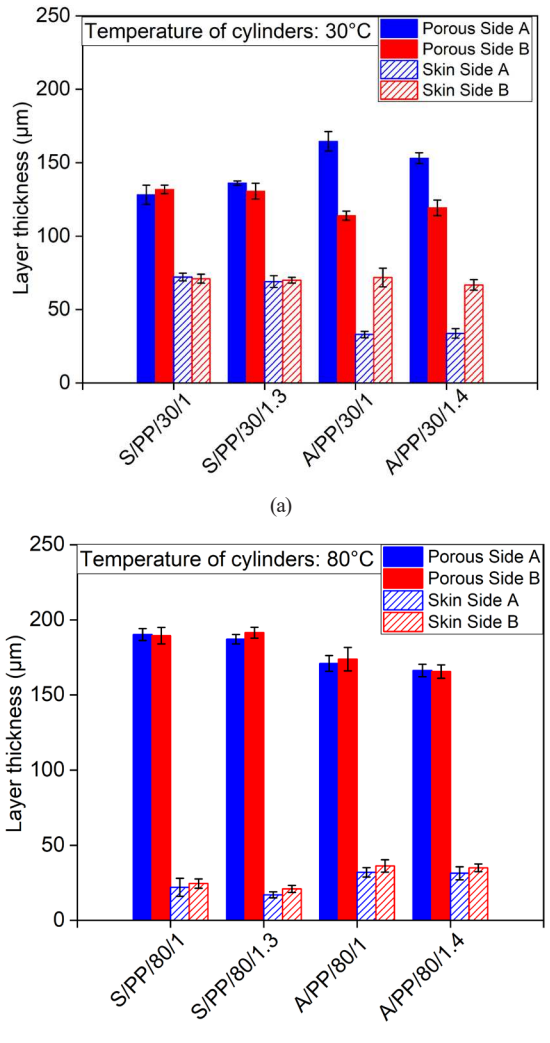

(a)

(b)

Fig. 5 Thickness of skin and porous layers of surface-treated samples cooled at (a) 30 °C and at (b) 80 °C

A (A/PP/30/1 and A/PP/30/1.4) did not show a core-shell–like structure that would differ from the others. The thickness of the porous layer increased, and the thickness of the skin layer decreased on side A.

Fig. 5 (b) shows the layer thicknesses of the samples cooled at 80 °C. In the case of samples where the original materials have a symmetrical structure (samples S/PP/80/1 and S/PP/80/1.3), layer thickness values on the opposite sides of the samples are the same. Contrary to the results obtained with cooling at 30 °C, the 80 °C–cooled samples, even in the case of the asymmetric extruded structure (sample A/PP/80/1 and A/PP/80/1.4), did not show asymmetric morphology after the solvent treatment. The skin and porous layers have the same thickness.

Regarding drawing speeds, we can conclude that its effect can be neglected on the final morphology – the thickness of the layers was similar.

The skin layer of samples cooled at 30 °C was thicker and the porous layer was thinner than those values of the samples cooled at 80 °C. No clear relationship can be established between the layer thicknesses of the samples and the drawing rate, regardless of the cooling rate in the investigated range.

After removing the skin layer, we evaluated the remaining surface morphology of the samples with spherulite size and water wetting behavior. As a reference, we also measured the wettability of extruded PP sheets, which had CA_{adv} of 102° and CA_{hyst} of 7°. The results are listed in Table 3.

The average size of the spherulites measured on the surface was in the range of 10 to 19 μm, regardless of the morphology structure of the extrudate which was subjected to the solvent treatment. The results indicate that most of the samples show superhydrophobic characteristics. In two cases (samples S/PP/80/1 and S/PP/80/1.3), some reduction can be observed. These weaker contact angle results can be attributed to the mechanical degradation during the removal of the skin layer. In addition to their superhydrophobicity, the samples also have water-repellent properties because the measured contact angle hysteresis is less than 10°.

Based on the investigation of extrusion parameters, the cooling rate at the cylinder has the primary effect on the thickness of the porous layer and the formation of the skin layer. On the other hand, we found that these processing parameters and methods have an almost negligible effect on the size of spherulites on the surface in the investigated range. According to the literature, it is expected that the dominant effect on wettability should be relevant to the spherulite size.

To quantify the skin layer removability, we measure the force required to remove the skin layer from the surface by peeling tests. The average tear force results are shown in Table 4.

Table 3 Surface wettability and spherulite sizes of the solvent-treated PP sheets

Samples	CA adv (°)	CAhyst (°)	Spherulite size (μm)
S/PP/30/1	152.2 ± 1.7	1.1 ± 0.7	21.4 ± 7.3
S/PP/80/1	144.6 ± 9.3	8.0 ± 2.6	15.4 ± 4.3
S/PP/30/1.3	147.1 ± 3.9	3.2 ± 4.3	19.8 ± 6.2
S/PP/80/1.3	148.7 ± 1.1	1.3 ± 0.4	15.3 ± 3.1
A/PP/30/1	153.6 ± 3.2	2.2 ± 1.4	13.1 ± 3.2
A/PP/80/1	151.1 ± 4.0	2.7 ± 1.7	10.8 ± 3.5
A/PP/30/1.4	150.8 ± 1.5	4.0 ± 1.2	13.1 ± 3.2
A/PP/80/1.4	155.8 ± 3.0	1.8 ± 0.3	13.7 ± 4.2

Table 4 Tear force of the skin layer of surface-treated sheets

Sample	Tear force (N)
S/PP/30/1	3.0 ± 1.0
S/PP/30/1.3	2.1 ± 0.7
S/PP/80/1	18.5 ± 4.6
S/PP/80/1.3	19.8 ± 4.1

The average tear force is a good indication that the skin peeling becomes increasingly difficult at higher cooling temperatures. A higher force was required to skin the samples cooled at 80 °C. Here we have to note that in the case of samples cooled at 80 °C, the average tear force does not reflect the detachment of the inhomogeneous skin layer from the surface. The inhomogeneous skin layer separation is shown in Fig. 6. The scattering of the results is well discernible on the blue straight and dash-dot curves.

Based on the extrusion parameters investigation, the cooling rate at the cylinder has the primary effect on the thickness of the porous layer and the formation of the skin layer. On the other hand, we found that these processing parameters and methods have an almost negligible effect on the size of spherulites on the surface in the investigated range. According to the literature, it is expected that the dominant effect on wettability should be relevant to the spherulite size.

Besides the processing conditions, the morphology of the final PP surface should be influenced by other factors, such as the composition of the material. To investigate the efficiency of this way of development in our solvent-treatment process, we prepared two compositions: 1. using a nucleating agent, 2. using of minor polymer com-ponent for blending.

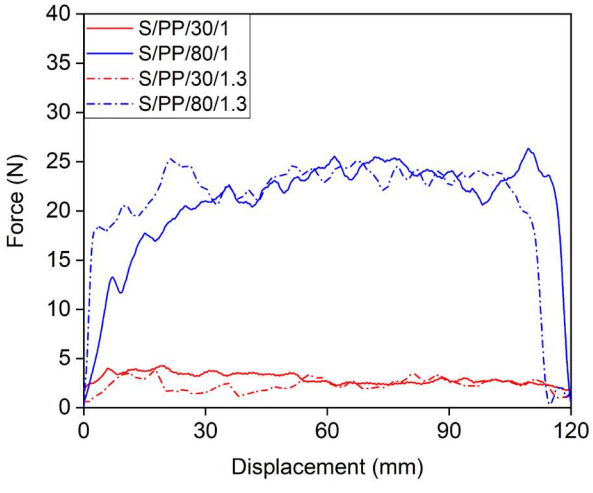

Fig. 6 Peeling test curves

In order to do this, we extruded nucleated PP and PP blends where the temperature of the cooling cylinders was set to 80 °C. Similar to the investigation of extrusion parameters, a POM study was carried out to analyze the cross-sectional morphology of the samples, which can be seen in Fig. 7.

The samples Fig. 7 (a)–(d) exhibited symmetrical structure, where spherulites formed along the cross-section due to the higher cooling temperature. In the case of A/PP-NA/80/1, the size of the spherulites is too small to be observed by POM, due to the effectiveness of the nucleating agent. The crystallinity of the samples was determined from DSC curves. The results are presented in Table 5.

There was no significant difference in the crystallinity; it varied between 33 and 35%. Meanwhile, the T_{cp} values increased slightly for blends and significantly for nucleated samples compared to neat PP. A notable increase in T_{cp} (126.7 °C) was observed in the nucleated PP samples, indicating the efficiency of nucleation.

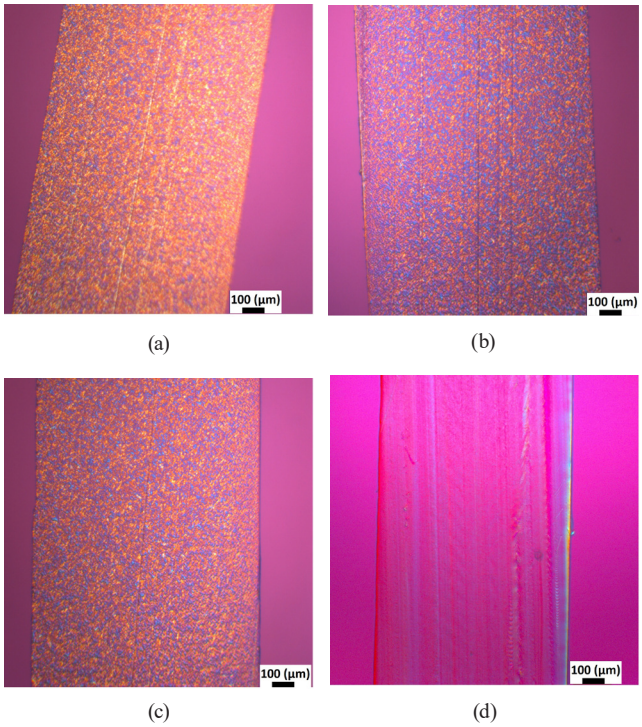

(a) (b)

(c) (d)

Fig. 7 POM images of the cross-section of extruded sheets cooled at 80 °C, where (a) is A/PP/80/1, (b) is A/PP-VP 792/80/1, (c) is A/PP-VP 703/80/1 and (d) A/PP-NA/80/1

Table 5 The value of crytallinity (X_C) and crystallization peak temperature (T_{cp}) obtained from DSC curves

Samples	X_C (%)	T_{cp} (°C)
A/PP/80/1	33.4	111.2
A/PP-VP 792/80/1	35.1	116.6
A/PP-VP 703/80/1	35.5	113.9
A/PP-NA/80/1	34.9	126.7

The morphology of the solvent-treated PP blends and the nucleated PP was investigated by cross-section SEM images and is shown in Fig. 8.

The symmetrical structure of the extruded sheets results in nearly the same thickness of the skin and porous layers on both sides of the samples. PP blends had the thickest porous layer, while the porous layer thickness of nucleated PP was nearly the same as in the case of neat PP.

The effect of APAOs and nucleating agent on the surface morphology of solvent-treated samples was investigated by SEM and can be seen in Fig. 9

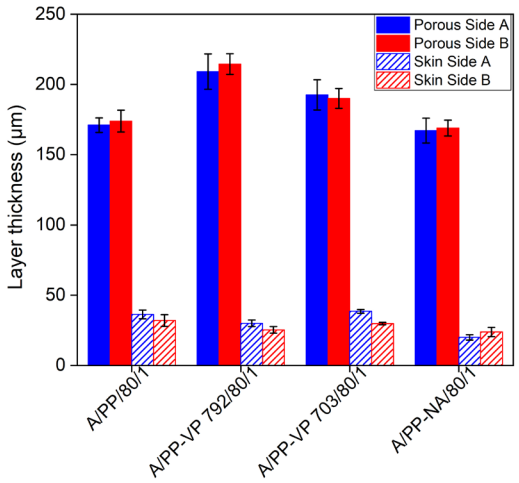

Fig. 8 Thickness of the skin and the porous layers of surface-treated PP blends and nucleated PP samples cooled at 80 °C

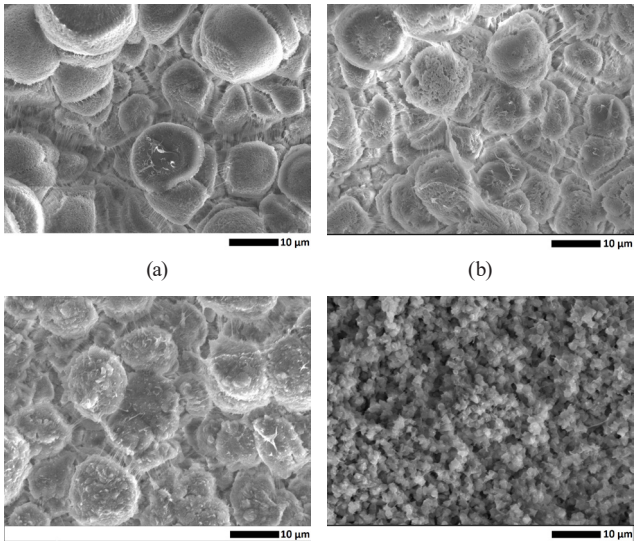

(a) (b)

(c) (d)

Fig. 9 SEM images of the surface of solvent-treated samples, where (a) is A/PP/80/1, (b) is A/PP-VP 792/80/1, (c) is A/PP-VP 703/80/1 and (d) A/PP-NA/80/1

Fig. 9 (a) shows the surface pattern of neat PP, where the surface is composed of spherulites. Fig. 9 (b) and (c) illustrates that the surface of spherulites of PP blends was more structured at the nanoscale level compared to the spherulites of the neat PP. However, a significant size change on a micro-scale did not occur. The surface of the nucleated PP (Fig. 9 (d)) was quite different from that of both neat PP and PP blends. Here, the size of the spherulites making up the microstructure of the surface was reduced considerably. In order to find a correlation between the micro- and nanostructural changes and superhydrophobicity, we measured the size of the spherulites and surface wettability. Table 6 contains these results.

The changes on the surfaces of the spherulites of PP blends did not change the contact angles appreciably. In contrast, the micro-size change on the surface of the nucleated samples resulting from the decrease in spherulite size led to a significant increase in contact angle, from 151 to 158° of CAadv. The change in the size of spherulites had a primary effect on wettability. The achieved nano-roughness modification did not have a significant impact on wettability.

According to the recommendations, VP 792 and VP703 might improve the elongation at break of the blend [34]. To evaluate the positive effect on the mechanical properties, we carried out tensile tests on both extruded and solvent-treated blends. The results are presented in Fig. 10.

Fig. 10 shows the results of tensile strength and elongation at break of extruded and solvent-treated samples. Based on the results of the extruded sheets, the addition of 10 wt% VP 703 increased elongation at break but did not change tensile strength. After the solvent treatment, the elongation at break of the samples was reduced compared to the extruded sheet, regardless of composition. In the case of solvent-treated PP blends, elongation at break was higher, while their tensile strength was lower than that of neat PP.

4 Discussion

If we want to test the reliability of our experiments on the effect of extrusion parameters, we can compare the cross-section images of the structure of extruded sheets

Table 6 Surface wettability and spherulite sizes of the solvent-treated PP composites

Samples	CAadv (°)	Spherulite size (μm)
F/80/1	151.1 ± 4.0	10.8 ± 3.5
F/PP 792/1	149.5 ± 6.7	12.6 ± 3.4
F/PP 703/1	148.7 ± 3.0	13.0 ± 2.9
S/PP NA/1	158.4 ± 3.2	2.5 ± 0.7

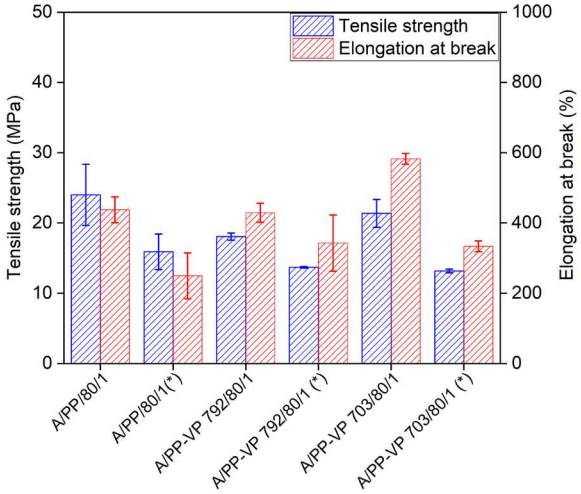

Fig. 10 Tensile strength and elongation at break of PP blends and nucleated PP in the samples; suffixes (*) refer to the solvent-treated samples

with some publications studying the effect of cooling temperature and pulling velocity. Macauley et al. [27] investigate the effect of various extrusion parameters on the morphological properties of PP, such as conveying cylinder temperature, pulling velocity, sheet thickness and melt temperature. For sheet extrusion, they used a tempered cylinder arrangement similar to the arrangement we used in our sheet extrusion. They extruded a PP sheet of 1.4 mm and demonstrated that a pulling velocity between 7 and 9 m/min could increase crystallinity, while a lower pulling velocity in the range of 3 to 5 m/min does not result in a crystallinity difference. With a higher velocity, the molecules are more prone to the orientation of the machine direction. They increased sheet thickness from 0.4 mm to 1.4 mm. The thinner sheet showed a lower level of crystallinity because of the greater cooling rates used on the sheet. They also varied the temperature of polymer melt and did not detect a significant influence on crystallinity. They detected an increase in overall crystallinity as the cooling temperature was increased from 30 °C to 80 °C. At the same time, they measured crystallinity separately inside the sheet and on both sides of the sheet that were in contact with the cooling cylinders. In this case, they found a significant difference in crystallinity along the cross-section of the sheet. On both sides of the sheet, the crystallinity was lower than the bulk phase at all cooling temperatures. They concluded that the temperature of cooling cylinders plays a significant role in the morphological characteristics of an extruded PP sheet.

Similar to Macauley and his coworkers' results, we found that the pulling velocity might have a minor effect on the morphology at the applied low velocity. By varying the temperature of cylinders, we also achieved morphology

changes in the cross-section of the samples from core–shell to fully spherulite structure. The significance of the temperature of the cylinder can also be recognized in film extrusion, where only one side of the sheet is connected to the cylinder. Here we can also follow the structural modification caused by the temperature of the cylinders.

A key step in achieving the superhydrophobic surface is to remove the skin layer after solvent treatment of the extruded sheets. Therefore, it is important to adjust the extrusion parameters so that the skin layer can be easily removed. The experiments showed that the skin layer must reach a minimum thickness to avoid the failure of the structured surface underneath the skin layer during the peeling step. The results show that the surface of the extruded sheets with a core–shell structure has a thicker skin layer than the spherulitic structure in cross-section. Thus, the structure of the extruded sheet cooled at different temperatures will affect the thickness of the skin layer. On the other hand, the cooling temperature of the cylinders does not change the size of the spherulites under the skin layer appreciably. With the applied solvent treatment method, we formed superhydrophobic characteristics on each extruded sample surface.

We also studied samples containing a minor polymer component or nucleating agent to investigate their role in surface morphological changes and indirectly on wetting behavior. The selected APAO grades (VP 703 and VP 792) differ in their molecular weight by order of magnitude. After solvent treatment and removal of the skin layer, spherulites crystallized on the surface of the PP blend. The size of the spherulites is almost the same size as the spherulites on the surface of neat PP. The surface of the spherulites is composed of micro-sized protuberances, so it may contribute to the modification of nano roughness, but it does not have a high impact on the surface wettability changes.

In the PP blends, 10 wt% APAO grades were mixed, and it did not lead to a notable change in surface wettability. Based on the SEM and surface wettability investigations, no differences can be found between PP blends of different molecular weights of APAO grades. In the future, it may be advisable to perform tests on PP blends containing different weight percents of APAOs.

Besides surface characterization, the mechanical properties of PP blends were also tested. From the comparison of extruded and solvent-treated samples, it is clearly visible that both tensile strength and elongation at break are reduced in each sample. During solvent treatment, the porous and skin layers are formed from the solvent-affected layer. In the porous layer, the spherulites are loosely connected to each other, so only the bulk phase, which is not affected by the solvent, will be the load-bearing part of the sample. From a mechanical properties point of view, it is favorable to minimize the thickness of the porous layer in the sample cross-section with the appropriate selection of extrusion and solvent treatment parameters.

The applied 10 wt% APAOs proved to be insufficient to achieve significant changes either in tensile strength or elongation at break. The positive effect of VP703 was detectable in elongation at break. It is supported by the work of Rioboo and his coworkers, where superhydrophobic surfaces were prepared from different compositions of PP blends by phase separation. They investigated the composition of blends to detect a change in wettability. Based on their study, if the percentage of PP exceeded a minimum level, the other polymer used in the PP blend had no effect on wettability. The transition percentage of PP was 30, 40 and 70% for polystyrene, polyvinyl acetate and polychloroprene blends, respectively [19].

In contrast to PP blends, a significant change in surface morphology and thus wettability can be achieved with nucleated PP. The nucleating agent, affected primarily the micro-roughness of the surface and reduced the size of the Spherulites from 10.8 μm to 2.5 μm, resulted in a large contact angle of 158.4° on the surface. Thus, the surface treatment of nucleated PP proved to be an effective way to change surface wettability significantly.

5 Conclusions

In this study the phase separation method we applied to create a superhydrophobic surface on PP sheets behaved differently depending on the morphology of the extruded sheet. We analyzed samples containing minor polymer components or nucleating agents to reveal their role in surface morphological changes and indirectly on wetting behavior. Based on the results, the following conclusions can be drawn.

The investigated cooling temperature of 30 and 80 °C led to two different structure formations along the cross-section of extruded samples. With 30 °C-cooling, a core-shell like structure was obtained, while with 80 °C, a fully spherulite structure developed in the cross-section of the samples. The results indicated that the effect of the applied pulling velocity of 1.0–1.4 m/min on the morphology of the extruded sheet was negligible.

We have found that the applied phase separation method is efficient for increasing hydrophobicity as water contact angles measured on the roughened surfaces were significantly higher (~150°) compared to the extruded sheet (102°). However, it showed different behaviors as a function of the morphology of extruded sheet.After phase separation, in the case of a core–shell-like structure, we received a thicker skin layer and thinner porous layer compared to the extruded sheets with a spherulite structure. To obtain a superhydrophobic surface, the skin layer is necessary to be peeled off from the surface. The skin layer must reach minimal thickness to be removed without damaging the surface structure beneath. However, our results showed that the structure of the extruded sheet does not have a significant effect on surface wettability.

For the modification of wettability, we investigated PP blends and nucleated PP. In the case of PP blends, the nano-structure of the surface was changed while the micro-structure remained almost the same. In the case of nucleated PP, the micro-structure was greatly modified. We measured a significant increase in contact angle (158°) in the case of nucleated samples. Our results indicate that to change surface wettability, we primarily have to modify the micro-structure on the surface structure created.

Acknowledgment

Supported by the KDP-2021 Program of the Ministry for Innovation and Technology from the source of the National Research, Development and Innovation Fund.

The research reported in this paper is part of project no. BME-NVA-02, implemented with the support provided by the Ministry of Innovation and Technology of Hungary from the National Research, Development and Innovation Fund, financed under the TKP2021 funding scheme.

References

[1] Darband, G. B., Aliofkhazraei, M., Khorsand, S., Sokhanvar, S., Kaboli, A. "Science and Engineering of Superhydrophobic Surfaces: Review of Corrosion Resistance, Chemical and Mechanical Stability", Arabian Journal of Chemistry, 13, pp. 1763–1802, 2020. https://doi.org/10.1016/j.arabjc.2018.01.013

[2] Quan, Y.-Y., Chen, Z., Lai, Y., Huang, Z.-S., Li, H. "Recent advances in fabricating durable superhydrophobic surfaces: a review in the aspects of structures and materials", Materials Chemistry Frontiers, 5(4), pp. 1655–1682, 2021. https://doi.org/10.1039/D0QM00485E

[3] Liravi, M., Pakzad, H., Moosavi, A., Nouri-Borujerdi, A. "A comprehensive review on recent advances in superhydrophobic surfaces and their applications for drag reduction", Progress in Organic Coatings, 140, 105537, 2020. https://doi.org/10.1016/j.porgcoat.2019.105537

[4] Ghasemlou, M., Daver, F., Ivanova, E. P., Adhikari, B. "Bio-inspired sustainable and durable superhydrophobic materials: from nature to market", Journal of Materials Chemistry A, 7(28), pp. 16643–16670, 2019. https://doi.org/10.1039/C9TA05185F

[5] Zhu, Q., Yu, Y., Wu, Q.-Y., Gu, L. "Construction of Renewable Superhydrophobic Surfaces via Thermally Induced Phase Separation and Mechanical Peeling", Chinese Journal of Chemical Physics, 30(2), pp. 219–224, 2017. https://doi.org/10.1063/1674-0068/30/cjcp1612235

[6] Kumar, A., Nanda, D. "Methods and fabrication techniques of superhydrophobic surfaces", In: Samal, S. K., Mohanty, S., Nayak, S. K. (eds.) Superhydrophobic Polymer Coatings, Elsevier, 2019, pp. 43–75. ISBN 978-0-12-816671-0 https://doi.org/10.1016/B978-0-12-816671-0.00004-7

[7] Wang, X., Pan, Y., Liu, X., Liu, H., Li, N., Liu, C., Schubert, D. W., Shen, C. "Facile Fabrication of Superhydrophobic and Eco-Friendly Poly(lactic acid) Foam for Oil–Water Separation via Skin Peeling", ACS Applied Materials & Interfaces, 11(15), pp. 14362–14367, 2019. https://doi.org/10.1021/acsami.9b02285

[8] Hao, Z., Chen, C., Shen, T., Lu, J., Yang, H. C., Li, W. "Slippery liquid-infused porous surface via thermally induced phase separation for enhanced corrosion protection", Journal of Polymer Science, 58(21), pp. 3031–3041, 2020. https://doi.org/10.1002/pol.20200272

[9] Tan, X., Rodrigue, D. "A Review on Porous Polymeric Membrane Preparation. Part II: Production Techniques with Polyethylene, Polydimethylsiloxane, Polypropylene, Polyimide, and Polytetrafluoroethylene", Polymers, 11(8), 1310, 2019. https://doi.org/10.3390/polym11081310

[10] Chatterjee, S., Das, P., Tripathy, U., Singh, B. P., Besra, L. "Development of polymer-based superhydrophobic coating on cloth", Bulletin of Materials Science, 43(1), 130, 2020. https://doi.org/10.1007/s12034-020-02103-9

[11] Erbil, H. Y., Demirel, A. L., Avcı, Y., Mert, O. "Transformation of a Simple Plastic into a Superhydrophobic Surface", Science, 299(5611), pp. 1377–1380, 2003. https://doi.org/10.1126/science.1078365

[12] Rasouli, S., Rezaei, N., Hamedi, H., Zendehboudi, S., Duan, X. "Superhydrophobic and superoleophilic membranes for oil-water separation application: A comprehensive review", Materials & Design, 204, 109599, 2021. https://doi.org/10.1016/j.matdes.2021.109599

[13] Hooda, A., Goyat, M. S., Pandey, J. K., Kumar, A., Gupta, R. "A review on fundamentals, constraints and fabrication techniques of superhydrophobic coatings", Progress in Organic Coatings, 142, 105557, 2020.
https://doi.org/10.1016/j.porgcoat.2020.105557

[14] Menyhárd, A., Suba, P., László, Zs., Fekete, H. M., Mester, Á. O., Horváth, Zs., Vörös, Gy., Varga, J., Móczó, J. "Direct correlation between modulus and the crystalline structure in isotactic polypropylene", eXPRESS Polymer Letters, 9(3), pp. 308–320, 2015.
https://doi.org/10.3144/expresspolymlett.2015.28

[15] Zhu, T., Cai, C., Guo, J., Wang, R., Zhao, N., Xu, J. "Ultra Water Repellent Polypropylene Surfaces with Tunable Water Adhesion", ACS Applied Materials & Interfaces, 9(11), pp. 10224–10232, 2017.
https://doi.org/10.1021/acsami.7b00149

[16] Hejazi, I., Hajalizadeh, B., Seyfi, J., Sadeghi, G. M. M., Jafari, S.-H., Khonakdar, H. A. "Role of nanoparticles in phase separation and final morphology of superhydrophobic polypropylene/zinc oxide nanocomposite surfaces", Applied Surface Science, 293, pp. 116–123, 2014.
https://doi.org/10.1016/j.apsusc.2013.12.112

[17] Zhao, J., Huang, Y., Wang, G., Qiao, Y., Chen, Z., Zhang, A., Park, C. B. "Fabrication of outstanding thermal-insulating, mechanical robust and superhydrophobic PP/CNT/sorbitol derivative nanocomposite foams for efficient oil/water separation", Journal of Hazardous Materials, 418, 126295, 2021.
https://doi.org/10.1016/j.jhazmat.2021.126295

[18] Zhang, C., Chen, W., Chen, J., Wu, X., Wang, X. "Thermally Stable Polypropylene Superhydrophobic Surface Due to the Formation of a Surface Crystalline Layer of Microsized Particles", The Journal of Physical Chemistry C, 123(37), pp. 23075–23081, 2019.
https://doi.org/10.1021/acs.jpcc.9b06842

[19] Rioboo, R., Demnati, I., Ali, M. A., Sevkan, R., De Coninck, J. "Superhydrophobicity of composite surfaces created from polymer blends", Journal of Colloid and Interface Science, 560, pp. 596–605, 2020.
https://doi.org/10.1016/j.jcis.2019.10.043

[20] Gengec, N. A., Cengiz, U., Erbil, H. Y. "Superhydrophobic perfluoropolymer/polystyrene blend films induced by non-solvent", Applied Surface Science, 383, pp. 33–41, 2016.
https://doi.org/10.1016/j.apsusc.2016.04.160

[21] Karger-Kocsis, J., Bárány, T. (eds.) "Polypropylene Handbook. Morphology, Blends and Composites", Springer Nature, 2019. ISBN 978-3-030-12903-3
https://doi.org/10.1007/978-3-030-12903-3

[22] Moore, E. P. "Polypropylene Handbook. Polymerization, Characterization, Properties, Processing, Applications", Hanser-Gardner Publications, 1996. ISBN 1-56990-208-9

[23] Zhao, J., Wang, G., Chen, Z., Huang, Y., Wang, C., Zhang, A., Park, C. B. "Microcellular injection molded outstanding oleophilic and sound-insulating PP/PTFE nanocomposite foam", Composites Part B: Engineering, 215, 108786, 2021.
https://doi.org/10.1016/j.compositesb.2021.108786

[24] Luo, C., Wang, X., Migler, K. B., Seppala, J. E. "Effects of feed rates on temperature profiles and feed forces in material extrusion additive manufacturing", Additive Manufacturing, 35, 101361, 2020.
https://doi.org/10.1016/j.addma.2020.101361

[25] Fischer, C., Leisen, C., Merken, D., Jungmeier, A., Drummer, D. "The Influence of Processing Temperature on Morphological and Tribological Properties of Injection-Moulded Microparts", Advances in Mechanical Engineering, 6, 218761, 2014.
https://doi.org/10.1155/2014/218761

[26] Li, M., Qi, Y., Zhao, Z., Xiang, Z., Liao, X., Niu, Y., Kong, M. "Morphology evolution and crystalline structure of controlled-rheology polypropylene in micro-injection molding", Polymers for Advanced Technologies, 27(4), pp. 494–503, 2016.
https://doi.org/10.1002/pat.3696

[27] Macauley, N. J., Harkin-Jones, E. M. A., Murphy, W. R. "The influence of extrusion parameters on the mechanical properties of polypropylene sheet", Polymer Engineering and Science, 38(4), pp. 662–673, 1998.
https://doi.org/10.1002/pen.10231

[28] Liparoti, S., Speranza, V., Sorrentino, A., Titomanlio, G. "Mechanical Properties Distribution within Polypropylene Injection Molded Samples: Effect of Mold Temperature under Uneven Thermal Conditions", Polymers, 9(11), 585, 2017.
https://doi.org/10.3390/polym9110585

[29] Way, J. L., Atkinson, J. R., Nutting, J. "The effect of spherulite size on the fracture morphology of polypropylene", Journal of Materials Science, 9(2), pp. 293–299, 1974.
https://doi.org/10.1007/BF00550954

[30] Liu, Z., Ren, L., Jing, J., Wang, C., Liu, F., Yuan, R., Jiang, M., Wang, H. "Fabrication of robust superhydrophobic organic-inorganic hybrid coating through a novel two-step phase separation method", Progress in Organic Coatings, 157, 106320, 2021.
https://doi.org/10.1016/j.porgcoat.2021.106320

[31] Li, C., Boban, M., Beebe, J. M., Bhagwagar, D. E., Liu, J., Tuteja, A. "Non-Fluorinated, Superhydrophobic Binder-Filler Coatings on Smooth Surfaces: Controlled Phase Separation of Particles to Enhance Mechanical Durability", Langmuir, 37(10), pp. 3104–3112, 2021.
https://doi.org/10.1021/acs.langmuir.0c03455

[32] Himma, N. F., Wardani, A. K., Wenten, I. G. "Preparation of Superhydrophobic Polypropylene Membrane Using Dip-Coating Method: The Effects of Solution and Process Parameters", Polymer-Plastics Technology and Engineering, 56(2), pp. 184–194, 2017.
https://doi.org/10.1080/03602559.2016.1185666

[33] Gee, D. R., Melia, T. P. "Thermal properties of melt and solution crystallized isotactic polypropylene", Macromolecular Chemistry and Physics, 132(1), pp. 195–201, 1970.
https://doi.org/10.1002/macp.1970.021320117

[34] Varga, L. J., Bárány, T. "Development of polypropylene-based single-polymer composites with blends of amorphous poly-alpha-olefin and random polypropylene copolymer", Polymers, 12(6), 1429, 2020.
https://doi.org/10.3390/polym12061429